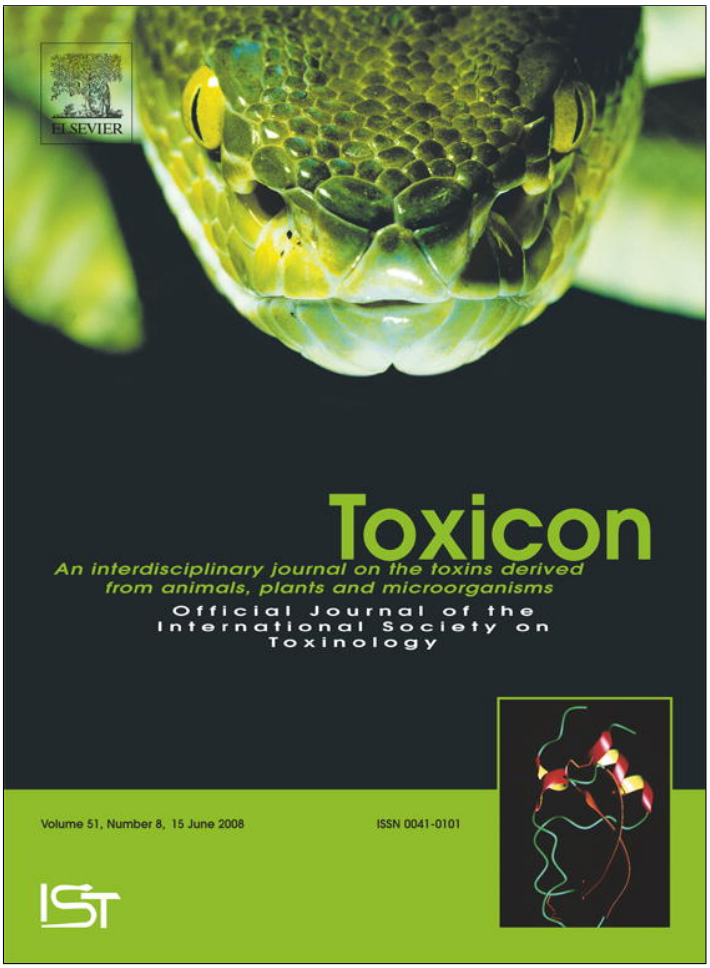

Toxicon 51 (2008) 1345–1356

Contents lists available at ScienceDirect

Toxicon

journal homepage: www.elsevier.com/locate/toxicon

Lysophospholipids prevent binding of a cytolytic protein ostreolysin to cholesterol-enriched membrane domains ☆

Helena H. Chowdhury [a,1], Katja Rebolj [b,1], Marko Kreft [a], Robert Zorec [a], Peter Maček [b], Kristina Sepčić [b,*]

[a] Laboratory of Neuroendocrinology—Molecular Cell Physiology, Faculty of Medicine, Institute of Pathophysiology, Slovenia & Celica Biomedical Center, University of Ljubljana, Proletarska 4, 1000 Ljubljana, Slovenia
[b] Department of Biology, Biotechnical Faculty, University of Ljubljana, Večna pot 111, 1000 Ljubljana, Slovenia

ARTICLE INFO

Article history:
Received 3 October 2007
Received in revised form
25 February 2008
Accepted 3 March 2008
Available online 18 March 2008

Keywords:
Cholesterol
Lipid raft
Membrane domains
Lysophospholipids
Pleurotus ostreatus
Pore-forming protein

ABSTRACT

Ostreolysin, a 15 kDa pore-forming protein from the oyster mushroom (*Pleurotus ostreatus*), binds specifically to cholesterol-enriched membrane domains existing in the liquid-ordered phase, and lyses cells and lipid vesicles made of cholesterol and sphingomyelin. We have monitored binding of sub-lytic concentrations of ostreolysin to membranes of Chinese Hamster Ovary cells and rat somatotrophs, using primary anti-ostreolysin and fluorescence-labeled secondary antibodies detected by confocal microscopy. Depletion of more than 40% membrane cholesterol content by methyl-β-cyclodextrin dramatically decreased ostreolysin binding. Immunostaining showed that ostreolysin is not co-localized with raft-binding proteins, cholera toxin B-subunit or caveolin, suggesting that natural membranes display heterogeneity of cholesterol-enriched raft-like microdomains. Impaired ostreolysin binding was also observed after treating the cells with lysophosphatidylinositol. Effects of lysophosphatidylinositol on binding of ostreolysin to immobilized large sphingomyelin/cholesterol (1/1, mol/mol) unilamellar vesicles were studied by a surface plasmon resonance technique. Injection of ostreolysin during the lysophosphatidylinositol dissociation phase showed an inverse relationship between ostreolysin binding and the quantity of lysophosphatidylinositol in the membranes of lipid vesicles. It was concluded that lysophospholipids prevent binding of ostreolysin to cell and to artificial lipid membranes resembling lipid rafts, by partitioning into the lipid bilayer and altering the properties of cholesterol-rich microdomains.

Abbreviations: CHO, Chinese Hamster Ovary cells; Chol, cholesterol; CT-B, Cholera toxin subunit B; DOPC, dioleoylphosphatidylcholine; DRMs, detergent-resistant membranes; FBS, fetal bovine serum; GPI, glycosylphosphatidylinositol; l_d, liquid-disordered; l_o, liquid-ordered; LP, lysophospholipid; LPC, lysophosphatidylcholine; LPI, lysophosphatidylinositol; LUVs, large unilamellar vesicles; MβCD, methyl-β-cyclodextrin; MLVs, multilamellar vesicles; Oly, ostreolysin; PC, phosphatidylcholine; POPC, palmitoyl-oleoylphosphatidylcholine; RU, resonance unit; S.E., standarad error; SM, sphingomyelin; SPR, surface plasmon resonance; SUVs, small unilamellar vesicles..

☆ *Ethical statement*: The protein used in this study was purified from edible oyster mushrooms (*Pleurotus ostreatus*, strain Plo5), that were taken from the ZIM collection of the Biotechnical Faculty, University of Ljubljana, Slovenia.

* Corresponding author. Tel.: +386 14233388; fax: +386 12573390.
E-mail address: kristina.sepcic@bf.uni-lj.si (K. Sepčić).

[1] These authors contributed equally to this study.

0041-0101/$ - see front matter © 2008 Elsevier Ltd. All rights reserved.
doi:10.1016/j.toxicon.2008.03.010

1. Introduction

According to the current model of cell membrane structure, certain membrane lipids, especially sterols, are responsible for the separation of membrane lipid domains into co-existing liquid-disordered (l_d) and liquid-ordered (l_o) domains (McConnell and Vrljic, 2003). The latter are the basis for formation of lipid rafts, cell membrane entities enriched in sphingolipids, cholesterol (Chol), and specific proteins (Pike, 2004). Rafts are involved in several important biological functions, such as exocytosis and endocytosis, signal transduction, pathogen entry, and attachment of various ligands (Edidin, 2003; London, 2002; Simons and Ikonen, 1997). They are believed to be transient, dynamic, and unstable membrane entities, which are stabilized on binding ligand molecules (Hancock, 2006; Kenworthy et al., 2000; Subczynski and Kusumi, 2003), and exist as nanoscale clusters (Hancock, 2006; Sharma et al., 2004) of various sizes (de Almeida et al., 2005).

Membrane domains in the l_o phase are more resistant to solubilization by detergents than the lipids in l_d domains (Lichtenberg et al., 2005) and, hence, lipid rafts are often operationally called detergent-resistant membranes (DRMs) (Simons and Ikonen, 1997). However, recent experimental data indicate that DRMs should not be assumed to describe biological rafts in size, structure, composition or even existence, as detergents themselves can induce the formation of ordered domains (Heerklotz, 2002; Lichtenberg et al., 2005).

The increasing amount of experimental evidence emphasizes the crucial biological roles of lipid rafts, thus increasing the need for new techniques and approaches to study these membrane microdomains. In particular, fluorescence-labeled cytolytic proteins that interact specifically with molecules enriched in lipid rafts are gaining interest. The best known, and the only commercially available raft-labeling agent, is the G_{M1} ganglioside-binding cholera toxin B subunit (CT-B) (Bacia et al., 2004). Two new candidates that have been proposed as possible selective markers for rafts are the pore-forming cytolysin, lysenin, whose truncated, non-toxic mutant recognizes sphingomyelin-enriched membrane domains specifically (Kiyokawa et al., 2005; Ishitsuka et al., 2005), and a protease-nicked and biotinylated non-toxic derivative of perfringolysin O (θ-toxin), that binds selectively to Chol-rich lipid rafts and DRMs (Ohno-Iwashita et al., 2004; Waheed et al., 2001). These proteins not only recognize the single lipid component, but are also sensitive to its distribution in the membrane and especially to its enrichment in lipid rafts.

Ostreolysin (Oly) is functionally a sterol-dependent cytolysin that binds specifically to SM membranes rich in Chol or other sterols, and to detergent-resistant fractions of cell membranes (Rebolj et al., 2006; Sepčić et al., 2004). This 15 kDa acidic protein is found in large amounts in young fruiting bodies of the edible mushroom *Pleurotus ostreatus* (Berne et al., 2002; Vidic et al., 2005), and belongs to the aegerolysin family of closely similar proteins that can be found in fungi, bacteria and plants (Berne et al., 2005). Cytolytic and hemolytic effects, that are the consequence of pore formation, are features of some aegerolysin-like proteins (Berne et al., 2002; Kumagai et al., 1999; Sakurai et al., 2004; Sepčić et al., 2003, 2004; Tomita et al., 2004), and can be responsible for their toxicity (Sakaguchi et al., 1975; Žužek et al., 2006). Aegerolysins appear to differ in their affinity for membrane acceptors. Pleurotolysin, an Oly isoform from *P. ostreatus*, was suggested to recognize sphingomyelin (SM) (Tomita et al., 2004), while Asp-hemolysin was proposed to bind lysophosphatidylcholine (LPC) specifically (Kudo et al., 2002). Our previous study on Oly binding and pore-forming properties revealed that the protein does not bind to pure SM or to other membrane lipids, but specifically senses membrane domains in which Chol is combined with either SM or fully saturated glycerophospholipids, suggesting its specific interaction with raft-like domains. This is supported by several lines of evidence. First, Oly can be found in isolated DRMs of both SM/Chol (1/1, mol/mol) vesicles and Chinese Hamster Ovary (CHO) cells (Sepčić et al., 2004). Secondly, permeabilization of SM/Chol vesicles by Oly appears only above 30 mol% Chol, the concentration at which this sterol induces the formation of a l_o-phase (de Almeida et al., 2003). It is interesting to note that between 30 and 40 mol% of Chol, the binding of Oly and its permeabilization of SM/Chol vesicles sharply increase from 0% to 22%, and from 0% to 90%, respectively (Rebolj et al., 2006; Sepčić et al., 2004). The interaction of Oly with Chol-enriched domains can be diminished or disrupted by the addition of mono- and di-unsaturated phosphatidylcholine (PC) (Sepčić et al., 2004), or by replacing Chol with other natural sterols or Chol derivatives (Rebolj et al., 2006). Furthermore, its hemolytic activity can be inhibited by the addition of micromolar concentrations of fatty acids and lysophospholipids, especially lysophosphatidylinositol (LPI), sphingosine-1-phosphate and lysophosphatidylcholine (Sepčić et al., 2003). Lysophospholipids (LPs) are single-chain, water-soluble surfactants that are found in small concentrations in lipid membranes, where they are synthesized de novo or are generated by enzymatic cleavage of glycerophospholipids and SM, and are released to regulate and maintain the organismal homeostasis (Gardell et al., 2006; Goetzl and An, 1998). Their signaling activity is mediated by the activation of transmembrane G-protein coupled receptors (Anliker and Chun, 2004). Thus, many LPs, especially lysophosphatidic acid and sphingosine-1-phosphate, affect fundamental cellular functions like proliferation, differentiation, survival, migration, adhesion, invasion and morphogenesis (Ishii et al., 2004). Impairment of their signaling functions is associated with several metabolic and physiological disorders (Gardell et al., 2006).

The aim of this work was to further investigate the interaction of Oly with Chol-rich raft-like membrane domains. Rabbit anti-Oly and fluorescent Alexa fluor 546-labeled secondary goat antibodies were used to monitor the binding of a sub-lytic concentration of Oly to membranes of CHO cells and rat somatotrophs, both under normal conditions and after treating the cells with methyl-β-cyclodextrin (MβCD) or lysophosphatidylinositol. Additionally, the effect of LPI on Chol/SM vesicles in

the l_o phase, and consequently on the binding of Oly, was studied in detail using surface plasmon resonance (SPR). We found that the binding of Oly to membranes of CHO cells is not uniform, but occurs in distinct domains. Oly binding is practically abolished on depletion of membrane Chol with MβCD. Since MβCD induces perturbation of membrane rafts and of the l_o phase, it is indicative that Oly binds specifically to Chol-rich raft-like microdomains. These membrane microdomains are, however, different from caveolae and from CT-B binding membrane domains, since no co-localization of Oly with caveolin or CT-B was observed. Decreased membrane-binding ability of Oly to the cells was also observed in the presence of LPI. As demonstrated by SPR and other studies, this lysophospholipid does not interact directly with Oly, suggesting that the inhibitory effect on Oly binding arises from partitioning of LPI into Chol-enriched membrane domains, hence affecting their properties required for binding of the protein.

2. Materials and methods

2.1. Materials

2.1.1. Proteins

Oly was isolated from fresh fruiting bodies of *P. ostreatus* as described (Berne et al., 2002). Its purity was checked by polyacrylamide gel electrophoresis. The protein concentration was determined spectrophotometrically using the BCA Protein Assay Reagent (Pierce, USA). After isolation, the protein was desalted and kept frozen (−20 °C) in aliquots in 140 mM NaCl, 1 mM EDTA, 20 mM Tris–HCl buffer, pH 8.0. Rabbit anti-Oly primary antibodies were prepared as described (Berne et al., 2002). Mouse monoclonal antibodies to caveolin 1 were obtained from Abcam (Cambridge, UK). Secondary Alexa Fluor 546 goat anti-rabbit IgG, Alexa Fluor 488 goat anti mouse IgG, and Vybrant® Alexa Fluor® 488 Lipid Raft Labeling Kit for labeling lipid rafts with CT-B were all from Invitrogen, Carlsbad, CA, USA.

2.1.2. Cell culture media

Ham's F12-K medium, fetal bovine serum (FBS), Dulbecco's Modified Eagle's Medium, Nutrient Mixture F-12 HAM, MEM Alpha Medium, D-glucose, and Hepes were from Sigma, St. Louis, MO, USA. L-glutamine and UltroserG were from Life Technologies, Gaithersburg, MD, USA.

2.1.3. Lipids and other chemicals

Bovine liver L-α-lysophosphatidylinositol (LPI), porcine brain SM and wool grease cholesterol were from Avanti Polar Lipids (Alabaster, USA); lysophosphatidycholine (LPC), calcein, Triton X-100, and MβCD were from Sigma (St. Louis, USA). Light Antifade Kit and Live/Dead Viability/Cytotoxicity kit were both from Invitrogen, Carlsbad, CA, USA. Waco Free Cholesterol C and Wako test Phospholipids B (990-54009) kits for enzymatic determination of lipid concentration were from Waco Chemicals GmbH, Germany.

2.2. Methods

2.2.1. Preparation of Chinese Hamster Ovary (CHO) cell line

CHO-K1 (Chinese Hamster Ovary cells; ATCC CRL-1721) were cultured in 25 cm^2 plastic tissue culture flasks at 37 °C, 5% CO_2 in Ham's F12-K medium supplemented with 10% FBS, 2 mM L-glutamine, 1 U/mL penicillin and 1 μg/mL streptomycin. Cells were subcultured at 80% confluence. One day before the experiment, the cells were trypsinized and seeded onto 22 mm glass cover slips coated with poly-L-lysine.

2.2.2. Cell culture of somatotrophs

Primary cell cultures of somatotrophs were isolated as described (Ben-Tabou et al., 1994) from the anterior lobe of pituitary glands of adult male rats (Wistar, 200–300 g). Cells were placed on poly-L-lysine-coated coverslips and incubated in a nutrient medium composed of 27% Dulbecco's modified Eagle's medium, 54% Nutrient Mixture F-12 HAM, 9% MEM Alpha Medium, 0.4% D-glucose, 25 mM Hepes, 2 mM L-glutamine and 3% UltroserG at 37 °C, 5% CO_2. Cells were used for immunocytochemistry 1–4 days following the plating of cells.

2.2.3. Preparation of lysophospholipids

Stock solutions of LPI or LPC (3 mM) in vesicle buffer (140 mM NaCl, 20 mM Tris–HCl buffer, pH 8.0) were prepared by sonication (Ultrasonic processor VCX 750, Sonics & Materials Inc., USA), applying 10 s pulses for 30 min (40% amplitude) at room temperature. Prior to use, the solutions were dissolved in vesicle buffer and equilibrated for at least 1 h.

2.2.4. Treatment of CHO cells

Before treatment with Oly, CHO cells were either starved, treated with MβCD or with different concentrations of LPI. Controls were treated only with Oly. *Starvation*: cells were serum-starved in growth medium without FBS for 48 h. *Treatment with MβCD*: cells were incubated with solutions of MβCD for 30 min at 37 °C; final concentrations of MβCD were 2, 5, 10, and 20 mM. *Treatment with LPI*: cells were incubated with solutions of LPI for 15 min on 37 °C; final concentrations of LPI were 0.48, 1.6, and 4.8 μM. *Treatment with Oly*: cells were washed with Earl's balanced salt solution (EBSS) and incubated with 67 nM Oly for 30 min at 37 °C. In the set of experiments with LPI, cells were not washed before treatment with Oly.

2.2.5. Immunostaining of cells

After fixing with paraformaldehyde, CHO cells were sequentially stained for 2 h with primary antibodies (rabbit polyclonal against Oly, 1:2500 or mouse monoclonal to caveolin 1, 1:500) and for 45 min with secondary antibodies (Alexa Fluor 546 goat anti-rabbit IgG, 1:500 or Alexa Fluor 488 goat anti mouse IgG, 1:500), diluted with 3% bovine serum albumin in phosphate buffered saline (PBS), and incubated at 37 °C. Cells were washed again with PBS and mounted on glass slides with the Light Antifade Kit. In the double staining protocol, cells were

treated sequentially with both primary antibodies and the corresponding secondary antibodies. Cells were labeled with CT-B according to the manufacturer's instructions, with a modified staining sequence: antibodies against CT-B in the double immunostaining with Oly were added at the end of the labeling. Binding specificity of primary antibodies was tested by labeling cells in the presence of secondary antibodies only.

2.2.6. Cell viability test

The percent cell viability was checked using the Live/Dead Viability/Cytotoxicity kit according to manufacturer's instructions. Cells were seeded on poly-L-lysine-coated cover slips, and stained with 2 mM calcein AM and 4 mM ethidium homodimer (EthD-1). In live cells, non-fluorescent cell-permeant calcein AM is converted to green fluorescing calcein by intracellular esterase activity. EthD-1 enters cells with damaged membranes with a 40-fold enhancement of red fluorescence on binding to nucleic acids. Cells were placed in a recording chamber on the confocal microscope (Zeiss LSM 510, Germany).

2.2.7. Confocal microscopy

Cells labeled with antibodies against Oly, caveolin 1, or CT-B were examined with an inverted Zeiss LSM 510 confocal microscope (oil-immersion objectives 63 × (NA 1.4) and 40 × (NA 1.3)). The conjugate Alexa Fluor 546 was excited by a He/Ne laser (543 nm) in combination with a long-pass filter with cut off below 560 nm. The conjugate Alexa Fluor 488 was excited by an argon laser (488 nm) in combination with a BP 505–530 nm emission filter. The fluorescence images of calcein-stained live cells and EthD-1-stained dead cells were acquired through a planapochromatic oil immersion objective 40 × (NA = 1.3) or 63 × (NA = 1.4). Calcein was excited by the 488 nm argon laser line and filtered with a BP 505–530 nm emission filter, and EthD-1 was excited by a He/Ne laser at 543 nm and filtered with the 560 nm low pass emission filter.

2.2.8. Cholesterol determination

Cholesterol content of membranes of CHO cells after different treatments was determined by extracting total lipids from ca. 4×10^6 cells as described (Sepčić et al., 2003), assuming that CHO cells possess approximatively 70% Chol associated to their plasma membranes (Warnock et al., 1993), and that MβCD depletes only Chol that is associated with them (Kilsdonk et al., 1995; Vrljic et al., 2005). Extracted total cell lipids were swollen in vesicle buffer, and vortexed vigorously to obtain multilamellar vesicles (MLVs). Small unilamellar vesicles (SUVs) were prepared by sonication (Ultrasonic processor VCX 750, Sonics & Materials Inc., USA), applying 10 s pulses for 30 min (40% amplitude) at room temperature. Cholesterol concentrations in SUV suspensions were determined colorimetrically using enzyme test. To calculate the degree of Chol depletion in treated CHO cells, the Chol membrane content of untreated cells was taken as 100%.

2.2.9. Preparation of liposomes

Chol/SM lipid vesicles in 1/1 molar ratio were formed by removing the organic solvents from the lipid solution in a round-bottomed flask by rotary evaporation and vacuum drying. Lipid film was swollen in either vesicle buffer or in 80 mM fluorescent dye calcein, at a final concentration range of 1 mg/mL, and vortexed vigorously to obtain MLVs. To obtain large unilamellar vesicles (LUVs) of a defined size, the suspension of MLVs was subjected to eight freeze-thawing cycles, and extruded through 0.05, 0.1, or 0.4 μm polycarbonate filters (Avestin, Ottawa, Canada) at 50 °C in a thermostated water bath. Liposomes with entrapped calcein were additionally separated from extra-vesicular calcein by gel filtration on a Sephadex G-50 (medium) column. Lipid concentrations of all suspensions were determined by measuring Chol and choline content by the enzymatic tests, as described in the previous paragraph.

2.2.10. Permeabilization of LUVs

Vesicle permeabilization was determined using a fluorescence microplate reader (Anthos Zenyth 3100, Anthos Labtec Instruments, Austria) with excitation and emission set at 485 and 535 nm, respectively. Fifty microliters of LPI in final concentrations 0–125 μM were dispensed onto a multiwell microplate, followed by 50 μL of Oly (8 μM) in vesicle buffer. Then, 100 μL of calcein-loaded Chol/SM (1/1, mol/mol) LUVs (100 nm) at a final concentration of 36 μM were added, and the release of calcein recorded for 1 h at 25 °C. In the control experiment, LPI was preincubated with 50 μL of vesicle buffer instead with Oly. One hundred percent calcein release was obtained by solubilization of LUVs with Triton X-100, 1 mM final concentration, and the percentage of calcein release was calculated for each as well as described (Menestrina, 1988).

2.2.11. Solubilization of LUVs by Triton X-100

Estimation of the insoluble DRM fraction in 100 nm LUVs, composed of SM and Chol in a 1/1 (mol/mol) ratio, was performed as described by Halling and Slotte (2004), by measuring the intensity of the scattered light following titration with Triton X-100 at 25 °C. The experiments were performed using a Jasco FP-750 spectrofluorometer (JASCO Ltd., Essex, UK) equipped with a water thermostated cell holder, using a 1 cm path length, magnetically stirred (830 rpm), quartz cuvette. Slit widths with a nominal band-pass of 5 nm were used for both excitation and emission. The excitation and emission wavelengths were set to 400 nm. The 0.5 mM LUVs suspensions in a quartz cuvette, with or without the addition of 4, 20, or 80 μM LPI, were titrated with 10 μL aliquots of a 10 mM Triton X-100 solution, all in vesicle buffer. The intensity of the scattered light was recorded 1 min after each addition of detergent. In the control experiments, Triton X-100 solution was replaced by buffer.

2.2.12. Surface plasmon resonance (SPR) measurements

Binding of Oly to immobilized Chol/SM (1/1, mol/mol) LUVs of different sizes was determined using a Biacore X

SPR apparatus with an L1 Sensor Chip (Biacore AB, Uppsala, Sweden) that retains intact liposomes on its lipophilic surface (Anderluh et al., 2005). All ligands and washing chemicals were prepared in degassed vesicle buffer previously filtered through a 0.22 μm filter. This was also used as running buffer. LUVs (0.5 mM) were deposited on the chip surface at a flow rate of 1 μL/min to achieve a response of 11,000–11,500 resonance units (RU). Loosely adsorbed lipid materials were washed out successively with 100 μL of 100 mM NaOH (30 μL/min) and with running buffer. Liposomes were then treated with 100 μL of 0.1 mg/mL bovine serum albumin (30 μL/min) to minimize non-specific binding of Oly to the microfluidic system. One hundred microliters of Oly (10, 20, or 40 μM in the running buffer) were injected over stably immobilized LUVs at a flow rate of 30 μL/min, followed by the continuous flow of the running buffer. Sensorgrams were recorded at 25 °C.

The effect of LPI on Oly binding was monitored by injecting 50 μL of 0.4, 0.8, or 1.6 μM LPI in the running buffer over the immobilized LUVs at a flow rate of 30 μL/min. This was followed by a continuous flow of running buffer to obtain dissociation kinetics. In order to estimate roughly the quantity (mol%) of LPI that was bound/inserted into LUV membranes, the LPI/LUV molar ratio was calculated from the SPR signal at different times during the dissociation kinetics, assuming that 1000 RU correspond to 1 ng of the compound bound (Anderluh et al., 2005). 100 μL of Oly (10, 20, or 40 μM in the running buffer) were injected at 30 μL/min over the LPI-pretreated LUVs at different times during the LPI dissociation. At the end of each experiment, the chip surface was purged with 100 μL of isopropanol: 40 mM NaOH (2:3) at 30 μL/min, and fresh LUVs were applied following the above procedure.

Controls were run by applying LPI or Oly alone to the chip surface, and bulk controls were run on immobilized vesicles with vesicle buffer alone. Also, LPI alone at 0.2 mM was applied to the chip surface, followed by the injection of Oly (20 μM). Sensorgrams were processed and evaluated using the BIAevaluation Version 3.2 software (Biacore AB, Uppsala, Sweden). In order to avoid the effect of LPI washing out from the membrane, the sensorgram for LPI alone was always subtracted from the sensorgram showing the Oly response. No fitting of the experimental curves was performed, due to the complex association/dissociation kinetics.

3. Results

3.1. Binding of ostreolysin to cells

The fluorescence signal, showing the distribution of Oly molecules bound to the membranes of CHO cells and rat somatotrophs, was not uniformly distributed over the cell surface, but was concentrated in many focal clusters, as visualized by confocal microscopy (Figs. 1A–C, left panels). This suggests that Oly recognizes distinct membrane areas at the surface of cells. The staining was specific since, in the absence of primary antibodies, no fluorescence signals could be detected (not shown).

Comparison of the Oly signal with that from caveolin, a 21 kDa integral membrane protein that is found in caveolae, uncoated round lipid raft invaginations in the plasma membrane (Pike and Miller, 1998), showed that the binding of the two proteins was very similar, non-uniform and dotted both on the membranes of CHO cells and somatotrophs (middle panels of Figs. 1A and B, respectively). However, the labeling patterns of the two proteins indicate that they were not co-localized (Figs. 1A and B, right panels). Our attempts to label the surface of CHO-cells with fluorescently labeled CT-B had failed (not shown), probably due to the absence of gangliosides at the membrane surface (Rosales Fritz et al., 1997), a characteristic of many clonal cells. Therefore, double staining of primary cultures of somatotrophs was performed. The fluorescence signals of Oly and CT-B showed patterns similar to those for Oly and caveolin on CHO cells and somatotrophs, with non-overlapping patterns of localization of the two proteins (Fig. 1C, right panel).

3.2. Effect of cholesterol depletion on ostreolysin binding to CHO cells

Our previous work with artificial lipid vesicles and CHO mutants with impaired Chol synthesis (Sepčić et al., 2004) suggested that the selective binding of Oly to membrane microdomains is Chol-dependent. To confirm this, Oly was applied to serum-starved cells, and to cells pretreated with MβCD, a water-soluble cyclic oligosaccharide acting as an extracellular Chol acceptor (Kilsdonk et al., 1995). The addition of 20 mM MβCD, that reduced the Chol membrane content by 43%, sharply diminished the binding of Oly to cells to only 2% (Figs. 2A and B). However, 10 mM MβCD, which resulted in depletion of membrane Chol by 35%, caused no significant reduction in the binding of Oly (Fig. 2B). Similarly, the ability of membranes to bind Oly was unchanged by a 9% reduction in Chol content caused by starvation (Fig. 2B).

3.3. Effect of lysophosphatidylinositol on ostreolysin binding to CHO cells

The addition of 4.8 μM LPI almost completely abolished the binding of Oly to CHO cells (Figs. 3A and B), in keeping with previous results that showed a decrease of hemolytic activity of Oly on addition of lysophospholipids (Sepčić et al., 2003). This concentration is well below the critical micellar concentration of LPI (70 μM) (Corda et al., 2002). On addition of LPI, the cells also adopted a more spherical shape (Fig. 3A, panels c and d), which is probably the consequence of the ability of LPs to rapidly partition to cell membranes, promoting their positive curvature (Alonso et al., 2000). The observed increased cell death rate (not shown) is also in accordance with the lytic effects of these natural amphiphiles (Davidsen et al., 2002).

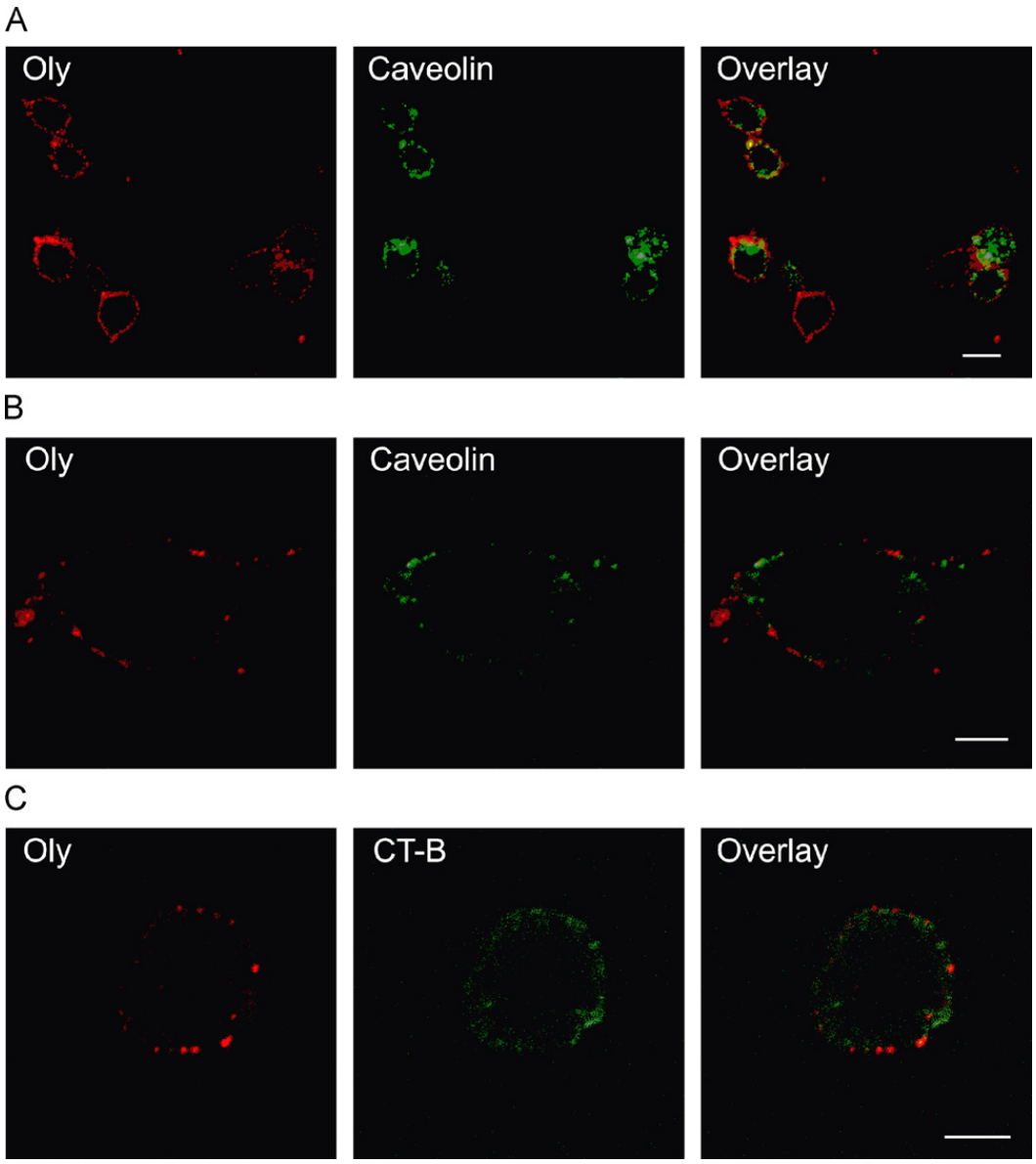

Fig. 1. Representative confocal images of CHO cells (A) and mouse somatotrophs (B, C), double-labeled with antibodies against Oly (left panels; red), and caveolin or CT-B (middle panels; green). Right hand panels show merged images of Oly and caveolin (A, B), or Oly and CT-B (C). Number of micrographs obtained and number of experiments are as follows: 8/2 (A), 12/2 (B), and 39/6 (C). Scale bars: 10 μm (A), and 5 μm (B and C). Cells were stained as described in Section 2.

3.4. Effect of lysophosphatidylinositol on ostreolysin binding to and permeabilization of SM/chol (1/1, mol/mol) vesicles

The direct interaction between LPI and LUVs composed of an equimolar mixture of SM and Chol was studied by SPR. At 25 °C, these vesicles exist in an l_o phase (Rebolj et al., 2006), and are very susceptible to Oly binding and lysis (Rebolj et al., 2006; Sepčić et al., 2004). Experiments with calcein-loaded LUVs showed that (i) LPI, at concentrations above 0.2 μM, inhibited the permeabilizing activity of Oly, and (ii) up to 100 μM LPI, Oly was unable to induce vesicle permeabilization (Fig. 4), indicating that, at the applied LUV/LPI ratios, the LUVs deposited on the L1 chip in SPR experiments were intact. Furthermore, titration of LUVs with Triton X-100 suggested that the addition of small amounts of LPI diminishes the proportion of insoluble DRM fraction in the tested LUVs (Fig. 5).

The association–dissociation kinetics of Oly interaction with LPI-treated LUVs immobilized on L1 chip, are shown in Fig. 6A. After the dissociation of LPI from the chip-immobilized LUVs, the RU signal always stabilized at the value of previously adsorbed LUVs (not shown), constituting additional evidence that the immobilized LUVs had remained intact through all the kinetics. The decrease of signal at the end of the dissociation phase would suggest the dissociation of LUVs from the chip surface, or their permeabilization.

The SPR experiments showed that the binding of Oly to lipid vesicles composed of an equimolar mixture of SM and Chol depends strongly on the amount of incorporated LPI, confirming the conclusions from the

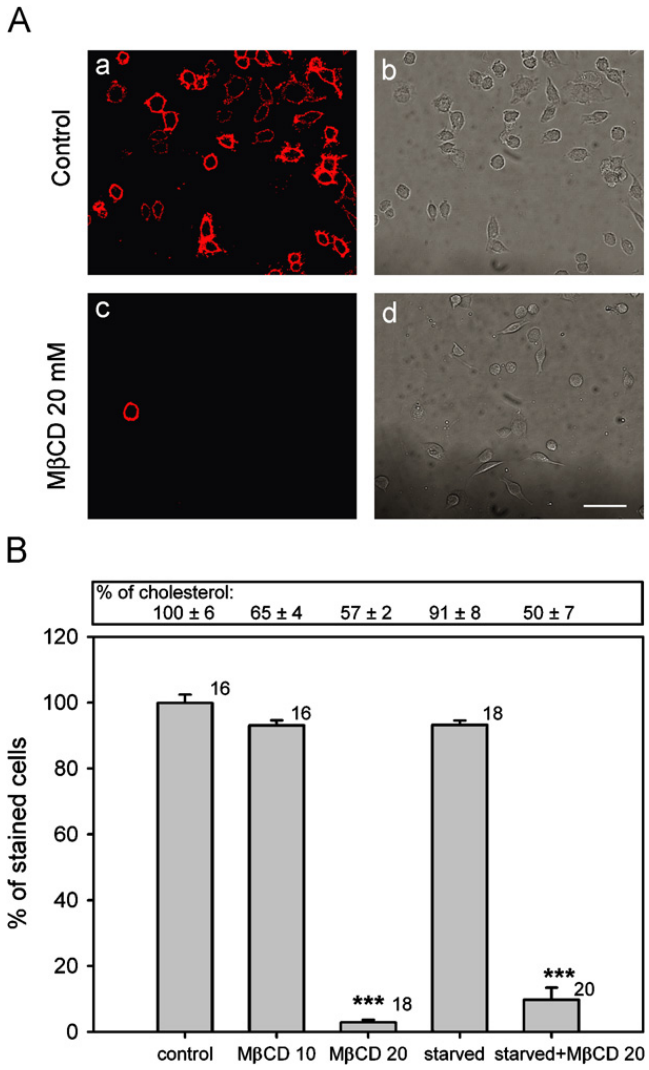

Fig. 2. Effect of methyl-β-cyclodextrin on ostreolysin binding to CHO cells. (A) Confocal images of untreated (a, b), or MβCD (20 mM) pretreated CHO cells (c, d). 16 control and 18 MβCD (20 mM) micrographs were analyzed, each set obtained from two experiments. Binding of Oly was assessed as described in Section 2. Panels a and c, immunofluorescence staining of Oly with a threshold set to 10% of the maximal fluorescence level; panels b and d, transmission micrographs of cells. Scale bar: 50 μm. (B) Percent of Oly-stained cells following starvation and pre-treatment of cells with MβCD. Bars represent mean values ± S.E. of 16–20 micrographs in two independent experiments. ***: $p \ll 0.001$. Numbers adjacent to error bars indicate the number of micrographs analyzed. The percentage of dead cells in each experiment (from left to the right) was 0.7, 0.2, 8.1, 5, and 4, respectively. The percentage of membrane Chol was estimated as described in Section 2.

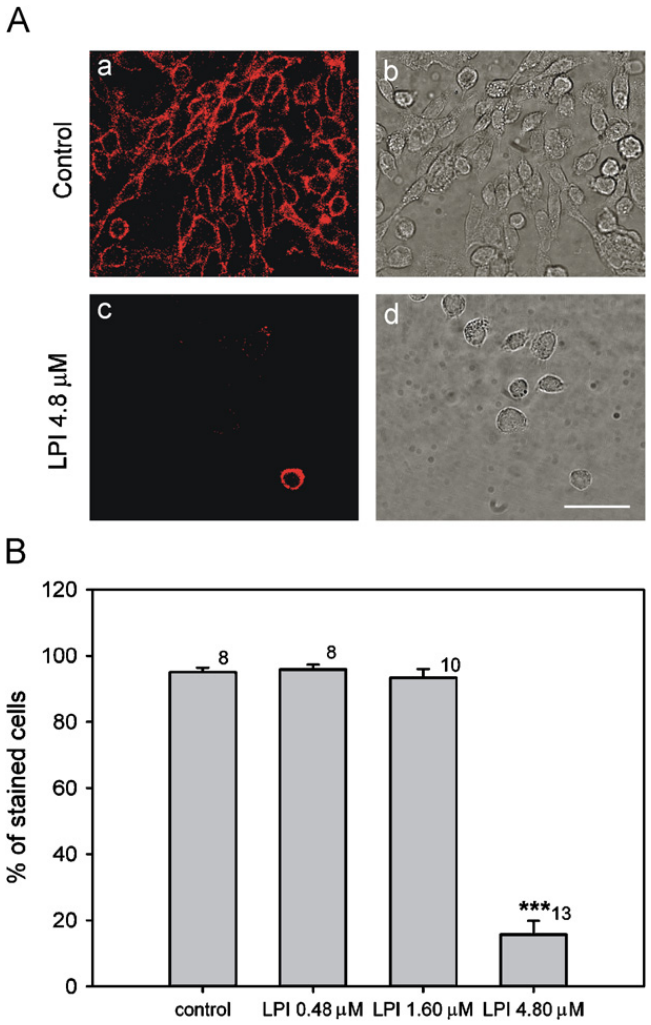

Fig. 3. Effect of lysophosphatidylinositol on Oly binding to CHO cells. (A) Confocal images of untreated (a, b), and LPI (4.8 μM) pretreated CHO cells (c, d). Binding of Oly was assessed as described in Section 2. Panels a and c, immunofluorescence staining of Oly; panels b and d, transmission micrographs of cells. Scale bar: 50 μm. (B) Percent of Oly-stained cells upon pretreatment with different concentrations of LPI. Bars represent mean values ± S.E. of two independent experiments. Numbers adjacent to error bars indicate numbers of micrographs analyzed. ***: $p \ll 0.001$. The percentage of dead cells in each experiment (from left to the right) was 0.6, 0.7, 0.2, and 3, respectively.

binding experiments on CHO cells (Fig. 3). The dissociation of LPI from LUVs is rather slow, taking 45 min for completion (Fig. 6A). This allows Oly to be injected at various times during the dissociation process. The binding signal of Oly is weak during the initial period of dissociation of LPI, increases on further dissociation from the vesicles, and is completely restored when the dissociation of LPI is complete (Figs. 6A and B). The dependence of Oly-binding on concentration of bound LPI in LUVs is shown in Fig. 7. It should be noted that, regardless of its maximal RU signal, the dissociation of Oly was never complete, suggesting that a fraction of the protein remained irreversibly bound to the membrane (Rebolj et al., 2006; Sepčić et al., 2004). The experiment was repeated also using LPC, which showed similar kinetics of association with and dissociation from the lipid vesicles, and behavior upon injection of Oly (not shown).

4. Discussion

Ostreolysin is shown to bind specifically to cholesterol-rich cell membrane microdomains of CHO cells, distinctive to cholera toxin-labeled or caveolin-rich lipid rafts. Binding of the protein is abolished by Chol depletion and by incorporation of lysophospholipids in the cell or artificial Chol-rich membranes, mimicking lipid rafts.

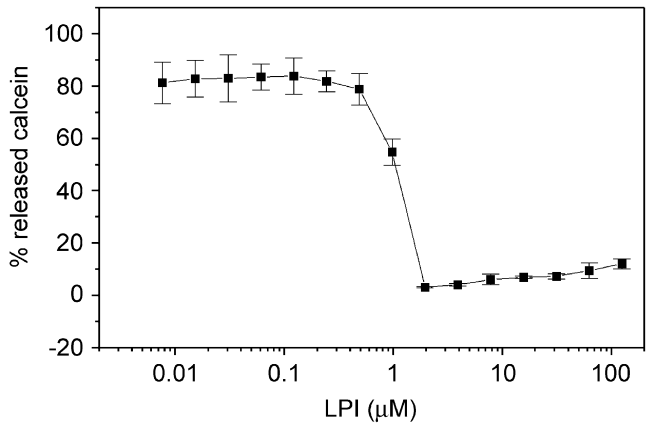

Fig. 4. Inhibition of ostreolysin-induced permeabilization of SM/Chol (1/1, mol/mol) LUVs by lysophosphatidylinositol. Ostreolysin (in the final concentration of 2 μM) was preincubated for 30 min at 25 °C with various amounts of sonicated LPI. Calcein-containing LUVs (36 μM) were added and the release of the fluorescent dye measured as described in Section 2. Each point represents the mean ± S.E. of three independent experiments. LPI did not induce the lysis of vesicles in the control experiment without Oly.

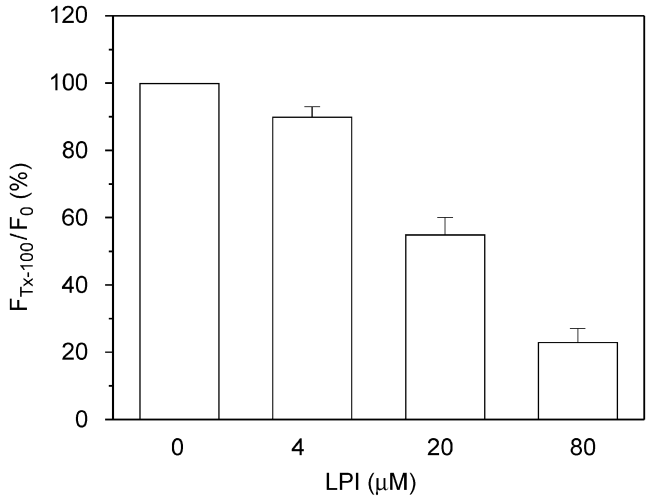

Fig. 5. Effect of lysophosphatidylinositol on solubilization of SM/Chol (1/1 molar ratio) LUVs by Triton X-100. The suspension of LUVs (0.5 mM), with or without different concentrations of LPI, was titrated with 10 μL aliquots of 10 mM Triton X-100, and the intensity of scattered light at λ_{exc} and $\lambda_{em} = 400$ nm was recorded 1 min subsequent to each detergent addition. F_{Tx-100} is the intensity of scattered light after addition of Triton X-100, and F_0 the intensity after addition of vesicle buffer (control). The measured values were normalized to the initial intensity (100%). Bars represent the F_{Tx-100}/F_0 values ± S.E. of two independent experiments after the cumulative addition of 1 mM Triton X-100.

4.1. Binding of Oly reveals heterogeneity of cholesterol-enriched membrane microdomains

Our previous search for the Oly membrane acceptor/receptor (Sepčić et al., 2003, 2004) showed that this cytolysin exerts its membrane activity only upon interaction with natural and artificial lipid membranes that are highly enriched in Chol and SM, or Chol and fully saturated glycerophospholipids. This suggests its specific interaction with lipid rafts, lateral heterogeneities in membranes of living cells enriched in SM, Chol, and specific proteins. Several cytolysins have been found to bind to DRM domains that fulfil the criteria of lipid rafts, interacting with different molecules that are enriched in these domains, like SM, Chol, ceramides, gangliosides, or the glycan core of GPI-anchored proteins (Alegre-Cebollada et al., 2006; Fivaz et al., 2001; Ishitsuka et al., 2005; Katagiri et al., 1999; Kenworthy et al., 2000; Miyata et al., 2002; Nagahama et al., 2003, 2004; Ohno-Iwashita et al., 2004; Schraw et al., 2002; Zhuang et al., 2002). Rafts were suggested to act as concentrating platforms that promote oligomerization of these toxins. In most of the cases, their binding can be abolished by membrane treatment with MβCD, which promotes the disruption of structural and functional integrity of low density membrane domains (Pike and Miller, 1998). Oly specific interaction with Chol/SM liposomes, its binding to DRMs of both cells and equimolar SM/Chol liposomes (Sepčić et al., 2004), as well as the inhibition of its binding after treatment of cell membranes with MβCD (Fig. 2), indicate Oly as a possible raft-binding protein. However, double immunolabeling experiments showed that the distribution of Oly did not coincide with the distribution of typical raft markers like caveolin and CT-B (Fig. 1). Similar lack of co-localization with caveolin was also reported for established raft-binding cytolysins like perfringolysin (Fujimoto et al., 1997) and cholera toxin (Kenworthy et al., 2000). Furthermore, different localization patterns of lysenin and CT-B were used as a basis for identifying functionally and structurally different raft-like regions of the plasma membrane (Kiyokawa et al., 2005). These data, combined with our results, reinforce the idea of a microheterogeneity of raft-like membrane microdomains (de Almeida et al., 2005; Hancock, 2006; Roper et al., 2000), that comprise at least two domain types: caveolin-containing (caveolae), and caveolin-lacking (rafts) (Pike, 2004).

The membrane-binding pattern of Oly generally resembles that of perfringolysin. Neither protein co-localizes with caveolin (Fujimoto et al., 1997; Fig. 1), both are proposed to sense Chol-enriched rafts (Ohno-Iwashita et al., 2004; Sepčić et al., 2004; this work), and neither binds to membranes after the considerable depletion of their Chol content (Fig. 2B; Waheed et al., 2001). However, in contrast to perfringolysin that can bind pure Chol (Palmer, 2004), Oly can interact with it only when the latter is combined with SM or fully saturated PC.

It appears that, compared to other raft-binding cytolysins, Oly needs higher local Chol concentration and higher degree of membrane ordering/structuring for effective binding and permeabilization. Several raft-binding cytolysins, even those that require Chol as their acceptor molecule, readily bind to and permeabilize vesicles composed of equimolar mixtures of SM and Chol with palmitoyl-oleoylphosphatidylcholine (POPC) or dioleoylphosphatidylcholine (DOPC), and can interact even with membranes composed of Chol and DOPC in the equimolar ratio (Alegre-Cebollada et al., 2006; Nagahama et al., 2004). This is not the case with Oly, in which the presence of mono- or di-saturated PC dramatically diminishes its membrane activity (Sepčić et al., 2004). These findings, supported by the fact that the presence of a certain degree of membrane ordering is not the sole

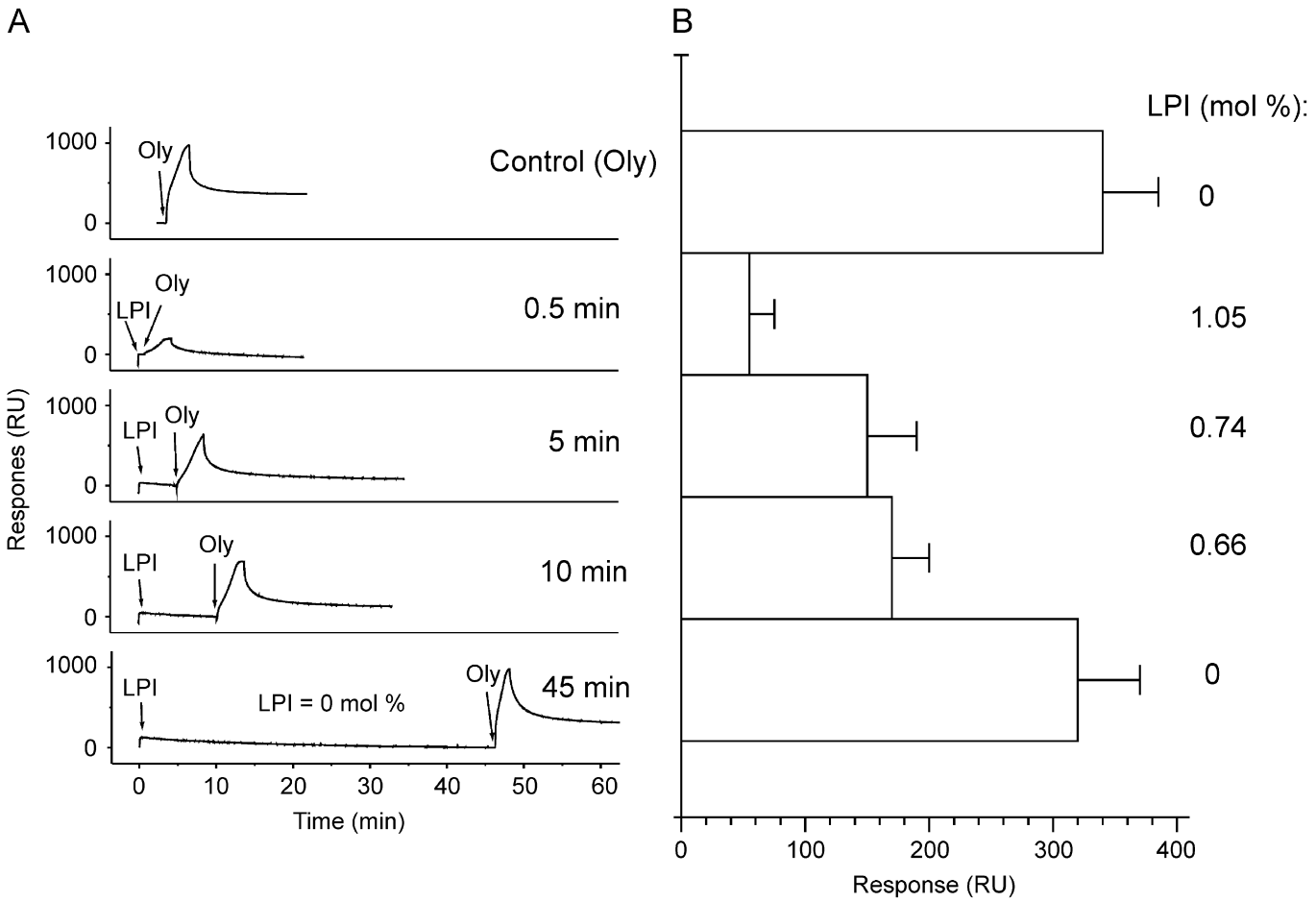

Fig. 6. Ostreolysin binding to SM/Chol (1/1, mol/mol) LUVs pretreated with 0.4 μM LPI. (A) Representative primary sensorgrams of LPI (0.4 μM) association with, and dissociation from immobilized LUVs. Fifty microliters of LPI (indicated by arrow) in 140 mM NaCl, 20 mM Tris–HCl, 1 mM EDTA, pH 8.0, were injected at 30 μL/min over 100 nm LUVs (0.5 mM) immobilized to the L1 chip at 25 °C. Oly was injected (arrow, 20 μM) in the same buffer at 30 μL/min at various times during the dissociation of LPI, as indicated at the right side of the panel. The control experiment indicates the Oly response on LUVs without addition of LPI. (B) Intensity of Oly binding on LPI-pretreated SM/Chol (1/1, mol/mol) LUVs, calculated from the primary sensorgrams corrected for the bulk effect. Oly was injected at different times during the LPI dissociation phase, as represented in the panel A. Each bar represents the mean maximal response (RU) of Oly ± S.E. of three separated experiments. The quantity of LPI (mol%), bound/inserted into LUV membranes at the time of Oly injection, was calculated from the SPR signal at different times during the dissociation kinetics, as described in Section 2.

prerequisite for Oly binding (Rebolj et al., 2006), suggest that Oly requires other structural/physical membrane features to fully exert its activity. One of its possible recognition sites could be small Chol clusters arranged in the plane of the membrane. These domains are Chol-dependent, as suggested by depletion experiments with MβCD (Fig. 2). The existence of small Chol clusters, whose stoichiometry varies with the Chol concentration, was recently suggested by molecular dynamics simulations of Chol/DPPC membranes (Pandit et al., 2007), as well as by other studies that proposed the formation of small condensed Chol and SM complexes in the rafts (Epand, 2003; Jacob and Mason, 2005). These clusters could act as docking sites for certain raft-binding cytolysins, including Oly. Along with this hypothesis, lysenin and perfringolysin were shown to recognize not only the sole lipid raft components (SM and Chol, respectively), but to specifically sense their distribution and clustering in the plane of membrane (Ohno-Iwashita et al., 2004; Ishitsuka et al., 2004; Kiyokawa et al., 2005).

Furthermore, it is suggestive that different raft-like domains require different Chol content to maintain their integrity (Roper et al., 2000). This could explain the sharp decrease in Oly binding after the depletion of Chol membrane content from 35% to 43% (Fig. 2), the phenomenon that was already observed during the monitoring of Oly membrane activity on Chol/SM liposomes with varying Chol content (Rebolj et al., 2006; Sepčić et al., 2004). Depletion of the threshold concentration of Chol could result in structural changes of the Chol-enriched microdomains, and in alterations of their distribution pattern in the plane of the membrane, preventing their recognition by Oly.

4.2. *Interaction of Oly with lipid membranes is prevented by increased content of membrane lysophospholipids*

The observed decreased binding of Oly to natural (Sepčić et al., 2003; Fig. 3) and artificial (Fig. 6) lipid membranes after their treatment with LPI could result because of (i) direct interaction of LPI with Oly, (ii) the increased positive membrane curvature induced by LPI, or (iii) the partitioning of LPI in Chol-rich membrane

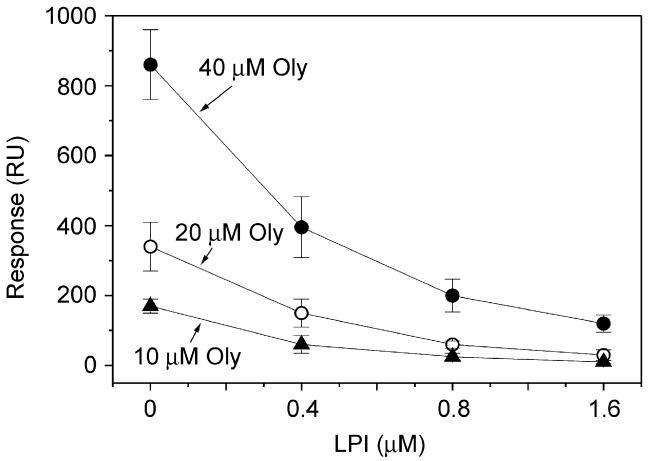

Fig. 7. Effect of LPI concentration on ostreolysin binding to SM/Chol (1/1, mol/mol) LUVs. Fifty microliter of LPI (0.4, 0.8, or 1.6 μM) in 140 mM NaCl, 20 mM Tris–HCl, 1 mM EDTA, pH 8.0, were injected at 30 μL/min over 100 nm LUVs (0.5 mM) immobilized to L1 chip at 25 °C. Oly in the same buffer, at various concentrations indicated on the graph, was injected at 30 μL/min 15 min after the start of the LPI dissociation phase. At this time, the RU signal dropped to approximately 50% of its maximal value. Each point represents the mean maximal response (RU) of Oly ± S.E. for three independent experiments.

domains and their consequent structural rearrangement and/or increase of membrane lateral pressure that abolishes the insertion of the protein. We were unable to detect the direct binding of Oly to LPs. Binding of LPC to Asp-hemolysin, another member of aegerolysins, was proved using ion-exchange chromatography (Kudo et al., 2002); however, our repetition of the same experiment using Oly combined either with LPC or LPI showed no interaction between the two molecules (Rebolj and Sepčić, unpublished data). On incubating with POPC lipid vesicles containing LPs, Oly never co-sedimented with them by ultracentrifugation, nor did it show any change in its intrinsic tryptophan fluorescence (Sepčić et al., 2003). Similar negative results were derived from a plethora of other experiments, e.g., from the absence of the signal on injecting Oly over the LPI-treated L1 chip surface in SPR experiments (this work; not shown), from native electrophoresis of preincubated LPs-Oly mixtures, from the absence of binding of Oly to PIP lipid strips (Invitrogen, Carlsbad, CA, USA) containing various LPs and phosphatidylinositols, and from the lack of change of the fluorescence spectrum on Oly titration with increasing concentrations of a synthetic fluorescent LP analogue dansyl-lysophosphatidylethanolamine (not shown). Further, some raft-binding toxins, like aerolysin, are susceptible to membrane curvature, and their binding can be decreased by the addition of lipids that favor the positive membrane curvature like LPs (Alonso et al., 2000). The decreased interaction of Oly with LPI-containing liposomes is unlikely to result from changes in the membrane curvature, as the same degree of Oly binding was observed in SPR experiments using liposomes of different sizes (0.05, 0.1, and 0.4 μm) (not shown). Altogether, our results strongly support the proposal that the reduced binding of Oly originates from structural changes of Chol-rich raft domains induced by LPs. As shown in Fig. 5, addition of LPI to LUVs in the l_o phase indeed facilitates the solubilization of a DRM fraction.

There have been reports that lysophospholipids (LPs) indeed could induce the disruption of lipid rafts and l_o domains. LPs and fatty acids can mediate membrane shape and function in membrane trafficking and exocytosis (Brown et al., 1993, Churchward et al., 2005), and their membrane partitioning depends strongly on the phase structure of the lipid membrane (Høyrup et al., 2001). When applied exogenously to lipid bilayers, LPs rapidly partition in the outer leaflet, and their flip-flop is of the order of hours in homogeneous bilayers (Bhamidipati and Hamilton, 1995). They were found to enter the l_o phase in artificial vesicles and cell rafts (Tanaka et al., 2004). When applied to liposomes having a heterogeneous membrane domain composition, they can induce shape changes, fission and budding (Tanaka et al., 2004; Staneva et al., 2005). These events appear on increasing the spontaneous curvature of the bilayer, thus decreasing the Gibbs free energy of the total system, and decreasing the boundary between the l_o and l_d phase. Recent investigations of the mode of action of anticancer alkyl-lysophospholipids present additional evidence that these compounds accumulate in rafts and modify their composition, leading to apoptosis (van der Luit et al., 2002; Zaremberg et al., 2005).

Our SPR experiments revealed real-time kinetics of LPI association with and dissociation from lipid bilayers with a composition resembling those of lipid rafts and l_o lipid domains. Increased membrane concentrations of LPI decrease the binding of Oly in the concentration-dependent manner. The dissociation kinetics, however, reveals that a fraction of Oly remains irreversibly bound to the membrane, suggesting that the membrane partition of LPI results in decreased number of Chol-enriched domains that fulfil the criteria for effective Oly binding.

5. Conclusions

First, the results indicate that Oly could be used to label cell membrane Chol-rich microdomains that are distinct from those visualized using cholera toxin B subunit or anti-caveolin antibodies. In addition, this finding supports the current view that cell lipid rafts are highly heterogeneous; those labeled by Oly are expected to be non-caveolar and to contain a relatively high proportion of Chol. In general, cytotoxicity limits the application of pore-forming proteins as probes for tracing membrane molecules in living cells; however, mutants of these toxins, devoid of their toxic properties, can be applied for confocal microscopy analysis as useful tools for studying the organization of lipid membranes and different functional pathways in the living cell.

Secondly, we find that the binding of Oly to cell and artificial lipid membranes that mimic lipid rafts is very sensitive to the membrane-partitioned lysophospholipids. Incorporation of LPs into the lipid bilayers markedly changes their properties, preventing the protein binding. Such behavior may apply generally to other

membrane-binding or even integral membrane proteins, harboring lipid rafts. Thus, LPs may exert dual regulatory activities in cells, via LP receptor-coupled processes and, directly, by changing properties of lipid rafts into which they are incorporated.

Acknowledgments

The authors gratefully acknowledge Ms. Irena Pavešić and Mr. Dejan Gmajner for excellent technical assistance; Ms. Sonja Grilc, Dr. Nina Vardjan, and Mr. Jernej Jorgačevski for the isolation of somatotroph cells; Prof. Roger Pain for critical reading of the manuscript, and the Slovenian Research Agency for the financial support (Grants P3 0381 310 and J1-6456).

References

Alegre-Cebollada, J., Rodriguez-Crespo, I., Gavilanes, J.G., del Pozo, A.M., 2006. Detergent-resistant membranes are platforms for actinoporin pore-forming activity on intact cells. FEBS J. 273, 863–871.

Alonso, A., Goni, F.M., Buckley, J.T., 2000. Lipids favoring inverted phase enhance the ability of aerolysin to permeabilize liposome bilayers. Biochemistry 39, 14019–14024.

Anderluh, G., Besenič ar, M., Kladnik, A., Lakey, J.H., Maček, P., 2005. Properties of nonfused liposomes immobilized on an L1 Biacore chip and their permeabilization by a eukaryotic pore-forming toxin. Anal. Biochem. 344, 43–52.

Anliker, B., Chun, J., 2004. Lysophospholipid G protein-coupled receptors. J. Biol. Chem. 279, 20555–20558.

Bacia, K., Scherfeld, D., Kahya, N., Schwille, P., 2004. Fluorescence correlation spectroscopy relates rafts in model and native membranes. Biophys. J. 87, 1034–1043.

Ben-Tabou, S., Keller, E., Nussinovitch, I., 1994. Mechanosensitivity of voltage-gated calcium currents in rat anterior pituitary cells. J. Physiol. 476, 29–39.

Berne, S., Križaj, I., Pohleven, F., Turk, T., Maček, P., Sepčić, K., 2002. *Pleurotus* and *Agrocybe* hemolysins, new proteins hypothetically involved in fungal fruiting. Biochim. Biophys. Acta 1570, 153–159.

Berne, S., Sepčić, K., Anderluh, G., Turk, T., Maček, P., Poklar Ulrih, N., 2005. Effect of pH on the pore forming activity and conformational stability of ostreolysin, a lipid raft-binding protein from the edible mushroom *Pleurotus ostreatus*. Biochemistry 44, 11137–11147.

Bhamidipati, S.P., Hamilton, J.P., 1995. Interactions of lyso 1-palmitoylphosphatidylcholine with phospholipids: a 13C and 31P NMR study. Biochemistry 34, 5666–5677.

Brown, S.D., Baker, B.L., Bell, J.D., 1993. Quantification of the interaction of lysolecithin with phosphatidylcholine vesicles using bovine serum albumin: relevance to the activation of phospholipase A2. Biochim. Biophys. Acta 1168, 13–22.

Churchward, M.A., Rogasevskaia, T., Höfgen, J., Bau, J., Coorssen, J.R., 2005. Cholesterol facilitates the native mechanism of Ca^{2+}-triggered membrane fusion. J. Cell Sci. 118, 4833–4848.

Corda, D., Iurisci, C., Berrie, C.P., 2002. Biological activities and metabolism of the lysophosphatidylinositols and glycerophosphoinositols. Biochim. Biophys. Acta 1582, 52–69.

Davidsen, J., Mouritsen, O.F., Jorgensen, K., 2002. Synergistic permeability enhancing effect of lysophospholipids and fatty acids on lipid membranes. Biochim. Biophys. Acta 1564, 256–262.

de Almeida, R.F.M., Fedorov, A., Prieto, M., 2003. Sphingomyelin/phosphatidylcholine/cholesterol phase diagram: boundaries and composition of lipid rafts. Biophys. J. 85, 2406–2416.

de Almeida, R.F., Loura, L.M., Fedorov, A., Prieto, M., 2005. Lipid rafts have different sizes depending on membrane composition: a time-resolved fluorescence resonance energy transfer study. J. Mol. Biol. 346, 1109–1120.

Edidin, M., 2003. The state of lipid rafts: from model membranes to cells. Annu. Rev. Biophys. Biomol. Struct. 32, 257–283.

Epand, R.M., 2003. Cholesterol in bilayers of sphingomyelin or dihydrosphingomyelin at concentrations found in ocular lens membranes. Biophys. J. 84, 3102–3110.

Fivaz, M., Abrami, L., Tsitrin, Y., van der Goot, F.V., 2001. Not as simple as just punching a hole. Toxicon 39, 1637–1645.

Fujimoto, T., Hayashi, M., Iwamoto, M., Ohno-Iwashita, Y., 1997. Cross-linked plasmalemmal cholesterol is sequestered to caveolae: analysis with a new cytochemical probe. J. Histochem. Cytochem. 45, 1197–1205.

Gardell, S.E., Dubin, A.E., Chun, J., 2006. Emerging medicinal roles for lysophospholipid signalling. Trends Mol. Med. 12, 65–75.

Goetzl, E.J., An, S., 1998. Diversity of cellular receptors and functions for the lysophospholipid growth factors lysophosphatidic acid and sphingosine 1-phospate. FASEB J. 12, 1589–1598.

Halling, K.K., Slotte, J.P., 2004. Membrane properties of plant sterols in phospholipid bilayers as determined by differential scanning calorimetry, resonance energy transfer and detergent-induced solubilization. Biochim. Biophys. Acta 1664, 161–171.

Hancock, J.F., 2006. Lipid rafts: contentious only from simplistic standpoints. Nat. Rev. Mol. Cell. Biol. 7, 456–462.

Heerklotz, H., 2002. Triton promotes domain formation in lipid raft mixtures. Biophys. J. 83, 2693–2701.

Høyrup, P., Davidsen, J., Jørgensen, K., 2001. Lipid membrane partitioning of lysolipids and fatty acids: effects of membrane phase structure and detergent chain length. J. Phys. Chem. B 105, 2649–2657.

Ishii, I., Fukushima, N., Ye, X., Chun, J., 2004. Lysophospholipid receptors: signalling and biology. Annu. Rev. Biochem. 73, 321–354.

Ishitsuka, R., Yamaji-Hasegawa, A., Makino, A., Hirabayashi, Y., Kobayashi, T., 2004. A lipid-specific toxin reveals heterogeneity of sphingomyelin-containing membranes. Biophys. J. 86, 296–307.

Ishitsuka, R., Sato, S.B., Kobayashi, T., 2005. Imaging lipid rafts. J. Biochem. 137, 249–254.

Jacob, R.F., Mason, R.P., 2005. Lipid peroxidation induces cholesterol domain formation in model membranes. J. Biol. Chem. 280, 39380–39387.

Katagiri, Y.U., Mori, T., Nakajima, H., Katagiri, C., Taguchi, T., Takeda, T., Kiyokawa, N., Fujimoto, J., 1999. Activation of Src family kinase yes induced by Shiga toxin binding to globotriaosyl ceramide (Gb3/CD77) in low density, detergent-insoluble microdomains. J. Biol. Chem. 274, 35278–35282.

Kenworthy, A.K., Petranova, N., Edidin, M., 2000. High-resolution FRET microscopy of cholera toxin B-subunit and GPI-anchored proteins in cell plasma membranes. Mol. Biol. Cell 11, 1645–1655.

Kilsdonk, E.P., Yancey, P.G., Stoudt, G.W., Bangerter, F.W., Johnson, W.J., Phillips, M.C., Rothblat, G.H., 1995. Cellular cholesterol efflux mediated by cyclodextrins. J. Biol. Chem. 270, 17250–17256.

Kiyokawa, E., Baba, T., Otsuka, N., Makino, A., Ohno, S., Kobayashi, T., 2005. Spatial and functional heterogeneity of sphingolipid-rich membrane domains. J. Biol. Chem. 280, 24072–24084.

Kudo, Y., Ootani, T., Kumagai, T., Fukuchi, Y., Ebina, K., 2002. A novel oxidized low-density lipoprotein binding protein, Asp-hemolysin, recognizes lysophosphatidylcholine. Biol. Pharm. Bull. 25, 787–790.

Kumagai, T., Nagata, T., Kudo, Y., Fukuchi, Y., Ebina, K., Yokota, K., 1999. Cytotoxic activity and cytokine gene induction of Asp-hemolysin to murine macrophages. Nippon Ishinkin Gakkai Zasshi 40, 217–222.

Lichtenberg, D., Goni, F.M., Heerklotz, H., 2005. Detergent-resistant membranes should not be identified with membrane rafts. Trends Biochem. Sci. 30, 430–436.

London, E., 2002. Insights into lipid raft structure and formation from experiments in model membranes. Curr. Opin. Struct. Biol. 12, 480–486.

McConnell, H.M., Vrljic, M., 2003. Liquid–liquid immiscibility in membranes. Annu. Rev. Biophys. Biomol. Struct. 32, 469–492.

Menestrina, G., 1988. *Escherichia coli* hemolysin permeabilizes small unilamellar vesicles loaded with calcein by a single-hit mechanism. FEBS Lett. 232, 217–220.

Miyata, S., Minami, J., Tamai, E., Matsushita, O., Shimamoto, S., Okabe, A., 2002. Clostridium perfringens epsilon-toxin forms a heptameric pore within the detergent-insoluble microdomains of Madin-Darby canine kidney cells and rat synaptosomes. J. Biol. Chem. 277, 39463–39468.

Nagahama, M., Hayashi, S., Morimitsu, S., Sakurai, N., 2003. Biological activities and pore formation of Clostridium perfringens beta toxin in HL 60 cells. J. Biol. Chem. 278, 36934–36941.

Nagahama, M., Yamaguchi, A., Hagiyama, T., Ohkubo, N., Kobayashi, K., Sakurai, N., 2004. Binding and internalization of Clostridium perfringens iota-toxin in lipid rafts. Infect. Immun. 72, 3275–4267.

Ohno-Iwashita, Y., Shimada, Y., Waheed, A.A., Hayashi, M., Inomata, M., Nakamura, M., Maruya, M., Iwashita, S., 2004. Perfringolysin O, a cholesterol-binding cytolysin, as a probe for lipid rafts. Anaerobe 10, 125–134.

Palmer, M., 2004. Cholesterol and the activity of bacterial toxins. FEMS Microbiol. Lett. 238, 281–289.

Pandit, S.A., Khelashvili, G., Jakobsson, E., Grama, A., Scott, H.L., 2007. Lateral organization in lipid-cholesterol mixed bilayers. Biophys. J. 92, 440–447.

Pike, L.J., 2004. Lipid rafts: heterogeneity on the high seas. Biochem. J. 378, 281–292.

Pike, L.J., Miller, J.M., 1998. Cholesterol depletion delocalizes phosphatidylinositol bisphosphate and inhibits hormone-stimulated phosphatidylinositol turnover. J. Biol. Chem. 273, 22298–22304.

Rebolj, K., Poklar Ulrih, N., Maček, P., Sepčić, K., 2006. Steroid structural requirements for interaction of ostreolysin, a lipid-raft binding cytolysin, with lipid monolayers and bilayers. Biochem. Biophys. Acta 1758, 1662–1670.

Roper, K., Corbeil, D., Huttner, W.B., 2000. Retention of prominin in microvilli reveals distinct cholesterol-based lipid micro-domains in the apical plasma membrane. Nat. Cell Biol. 2, 582–592.

Rosales Fritz, V.M., Daniotti, J.L., Maccioni, H.J., 1997. Chinese hamster ovary cells lacking GM1 and GD1a synthesize gangliosides upon transfection with human GM2 synthase. Biochim. Biophys. Acta 1354, 153–158.

Sakaguchi, O., Shimada, H., Yokota, K., 1975. Purification and characteristics of hemolytic toxin from Aspergillus fumigatus. Jpn. J. Med. Sci. Biol. 28, 328–331.

Sakurai, N., Kaneko, J., Kamio, Y., Tomita, T., 2004. Cloning, expression, and pore-forming properties of mature and precursor forms of pleurotolysin, a sphingomyelin-specific two-component cytolysin from the edible mushroom *Pleurotus ostreatus*. Biochim. Biophys. Acta 1679, 65–73.

Schraw, W., Li, Y., McClain, M.S., van der Goot, F.G., Cover, T.L., 2002. Association of Helicobacter pylori vacuolating toxin (VacA) with lipid rafts. J. Biol. Chem. 277, 34642–34650.

Sepčić, K., Berne, S., Potrich, C., Turk, T., Maček, P., Menestrina, G., 2003. Interaction of ostreolysin, a cytolytic protein from the edible mushroom *Pleurotus ostreatus*, with lipid membranes and modulation by lysophospholipids. Eur. J. Biochem. 270, 1199–1210.

Sepčić, K., Berne, S., Rebolj, K., Batista, U., Plemenitaš, A., Šentjurc, M., Maček, P., 2004. Ostreolysin, a pore-forming protein from the oyster mushroom, interacts specifically with membrane cholesterol-rich lipid domains. FEBS Lett. 575, 81–85.

Sharma, P., Varma, R., Sarasij, R.C., Ira, Gousset, K., Krishnamoorthy, G., Rao, M., Mayor, S., 2004. Nanoscale organization of multiple GPI-anchored proteins in living cell membranes. Cell 116, 577–589.

Simons, K., Ikonen, E., 1997. Functional rafts in cell membranes. Nature 387, 569–572.

Staneva, G., Seigneuret, M., Koumanov, K., Trugnan, G., Angelova, M.I., 2005. Detergents induce raft-like domains budding and fission from giant unilamellar heterogeneous vesicles: a direct microscopy observation. Chem. Phys. Lipids 136, 55–66.

Subczynski, W.K., Kusumi, A., 2003. Dynamics of raft molecules in the cell and artificial membranes: approaches by pulse EPR spin labeling and single molecule optical microscopy. Biochim. Biophys. Acta 1610, 231–243.

Tanaka, T., Sano, R., Yamashita, Y., Yamazaki, M., 2004. Shape changes and vesicle fission of giant unilamellar vesicles of liquid-ordered phase membrane induced by lysophosphatidylcholine. Langmuir 20, 9526–9534.

Tomita, T., Noguchi, K., Mimuro, H., Ukaji, F., Ito, K., Sugawara-Tomita, N., Hashimoto, Y., 2004. Pleurotolysin, a novel sphingomyelin-specific two-component cytolysin from the edible mushroom *Pleurotus ostreatus*, assembles into a transmembrane pore complex. J. Biol. Chem. 279, 26975–26982.

van der Luit, A.H., Budde, M., Ruurs, P., Verheij, M., Blitterswijk, W.J., 2002. Alkyl-lysophospholipid accumulates in lipid rafts and induces apoptosis via raft-dependent endocytosis and inhibition of phosphatidylcholine synthesis. J. Biol. Chem. 277, 39541–39547.

Vidic, I., Berne, S., Drobne, D., Maček, P., Frangež, R., Turk, T., Štrus, J., Sepčić, K., 2005. Temporal and spatial expression of ostreolysin during development of the oyster mushroom (*Pleurotus ostreatus*). Mycol. Res. 109, 377–382.

Vrljic, M., Nishimura, S.Y., Moerner, W.E., McConnell, H.M., 2005. Cholesterol depletion suppresses the translational diffusion of class II major histocompatibility complex proteins in the plasma membrane. Biophys. J. 88, 334–347.

Waheed, A.A., Shimada, Y., Heijnen, H.F., Nakamura, M., Inomata, M., Hayashi, M., Iwashita, S., Slot, J.W., Ohno-Iwashita, Y., 2001. Selective binding of perfringolysin O derivative to cholesterol-rich membrane microdomains (rafts). Proc. Nat. Acad. Sci. USA 98, 4926–4931.

Warnock, D.E., Roberts, C., Lutz, M.S., Blackburn, W.A., Young, W.W., Baenziger, J.U., 1993. Determination of plasma membrane lipid mass and composition in cultured Chinese Hamster Ovary cells using high gradient magnetic affinity chromatography. J. Biol. Chem. 268, 10145–10153.

Zaremberg, V., Gajate, C., Cacharro, L.M., Mollinedo, F., McMaster, C.R., 2005. Cytotoxicity of an anti-cancer lysophospholipid through selective modification of lipid raft composition. J. Biol. Chem. 280, 38047–38058.

Zhuang, M., Oltean, D.I., Gomez, I., Pullikuth, A.K., Soberon, M., Bravo, A., Gill, S.S., 2002. *Heliothis virescens* and *Manduca sexta* lipid rafts are involved in Cry1A toxin binding to the midgut epithelium and subsequent pore formation. J. Biol. Chem. 277, 13863–13872.

Žužek, M.C., Maček, P., Sepčić, K., Cestnik, V., Frangež, R., 2006. Toxic and lethal effects of ostreolysin, a cytolytic protein from edible oyster mushroom (*Pleurotus ostreatus*), in rodents. Toxicon 48, 264–271.